THE ASTROPHYSICAL JOURNAL, 462:1–12, 1996 May 1

PLANETARY NEBULAE AS STANDARD CANDLES. X. TESTS IN THE COMA I REGION

GEORGE H. JACOBY
Kitt Peak National Observatory, National Optical Astronomy Observatories, P.O. Box 26732, Tucson, AZ 85726;
gjacoby@noao.edu

ROBIN CIARDULLO[1,2]
Department of Astronomy and Astrophysics, Penn State University, 525 Davey Lab, University Park, PA 16802;
rbc@astro.psu.edu

AND

WILLIAM E. HARRIS[1]
Department of Physics and Astronomy, McMaster University, Hamilton, Ontario L8S 4M1, Canada;
harris@physun.physics.mcmaster.ca
Received 1995 September 8; accepted 1995 November 9

ABSTRACT

We present the results of an [O III] $\lambda5007$ survey for planetary nebulae (PNs) in three galaxies of the Coma I group: NGC 4278 (Hubble type E1), NGC 4494 (E1), and NGC 4565 (edge-on Sb). Using the planetary nebula luminosity function (PNLF), we derive distances to NGC 4494 (12.8 ± 0.9 Mpc), NGC 4565 ($10.5^{+0.8}_{-1.0}$ Mpc), and NGC 4278 ($10.2^{+0.7}_{-1.0}$ Mpc). The larger distance for NGC 4494 is significant beyond the 99% confidence level when the common systematic errors in all three distances are removed. This agrees with the results of the globular cluster luminosity function and surface brightness fluctuation methods, both of which place NGC 4565 in front of NGC 4494. The large separation is also consistent with the results of Virgocentric flow models, which predict triple-valued solutions to the Hubble flow in that direction.

Our planetary nebula survey of the small elliptical NGC 4278 also reveals two [O III] $\lambda5007$ sources more luminous than the nominal limit of the PNLF. Both objects can be excluded a priori from the list of PN candidates: one is quite bright in Hα, the other is marginally resolved. Nevertheless, the existence of these objects in an otherwise normal elliptical galaxy poses a potential problem for the PNLF technique. We discuss the possible origins of objects brighter than the PNLF cutoff and consider one way in which their existence might be incorporated into PNLF distance measurements.

Subject headings: distance scale — galaxies: clusters: individual (Coma I) — galaxies: distances and redshifts — planetary nebulae: general

1. INTRODUCTION

The acceptance of any extragalactic distance indicator demands that it be tested for the presence of systematic errors. One of the simplest of these errors to understand may occur when viewing galaxies with differing Hubble types. An indicator that works within a spiral galaxy may not necessarily work the same way in an elliptical, due to differences in the underlying stellar population or mass distribution. Evidence for such an effect has been seen in the magnitudes of Type Ia supernovae (Hamuy et al. 1995) and for the globular cluster luminosity function (GCLF; Fleming et al. 1995). Since distance indicators such as the GCLF, the planetary nebula luminosity function (PNLF), surface brightness fluctuations (SBF), novae, and Type Ia supernovae are all used in early-type galaxies, but calibrated in spirals (via Cepheids), it is exceedingly important that tests for systematic errors of this type be performed.

There are two ways to search for such biases. The first technique is purely internal: distance estimates can be made to elliptical and spiral galaxies within a common, compact group. As long as there is no morphological segregation, an error-free indicator will yield similar distances to both types of galaxies. Since spiral galaxies are not always intermixed spatially with ellipticals, this test may occasionally yield a false result. However, if enough galaxy groups are analyzed, then the effects of morphological segregation should be reduced statistically.

The second method for detecting systematic distance errors is through external comparisons with the results of other methods. If the residuals between one distance indicator and another show a systematic trend with Hubble type, then it is likely that at least one of the methods is biased. Since no distance indicator is perfect, comparisons of this kind must assume that the errors of one method are uncorrelated with those of the other. Fortunately, this is usually a good assumption, especially since the physics underlying the most popular distance indicators are vastly different from one another (see Jacoby et al. 1992).

In this paper, we use a nearby, well-mixed group of galaxies in Coma I to examine the PNLF method for the presence of a spiral–elliptical systematic error. This group has long been recognized as a fertile proving ground for distance indicators, as it contains several spiral and E/S0 galaxies within a $\sim 1.8 \times 0.8$ Mpc elliptical region (de Vaucouleurs 1975). Moreover, two of the galaxies in the group, the E1 galaxy NGC 4494 and the giant edge-on spiral NGC 4565, have recently been measured with the SBF (Simard & Pritchet 1994) and GCLF (Fleming et al. 1995) techniques. This has turned the area into one of the best locations for performing intercomparisons between different standard candles. By adding our PNLF measurements to those of the SBF and GCLF techniques, we can test for the systematic

[1] Visiting Astronomer, Kitt Peak National Observatory, National Optical Astronomy Observatories, which is operated by the Association of Universities for Research in Astronomy, Inc., under cooperative agreement with the National Science Foundation.

[2] NSF Young Investigator.

errors in all three techniques and quantitatively assess the accuracy of each method.

In § 2 of this paper, we describe our observations of three galaxies in the Coma I cloud, NGC 4494, NGC 4565, and the small E1 elliptical NGC 4278, and present measurements of 255 newly identified PN candidates, including two "overluminous" objects. In §§ 3 and 4, we present our PNLF distances to these galaxies and find support for the SBF and GCLF contention that the group has a substantial line-of-sight thickness and thus is not as well mixed as originally believed. We conclude by discussing the possible origins of the overluminous sources and considering a modified PNLF law that takes into account the existence of objects brighter than the nominal PNLF cutoff.

2. OBSERVATIONS

Our observations were obtained in the spring of 1992 and 1995 with the prime focus of the Kitt Peak 4 m telescope and the T2KB 2048 × 2048 Tektronix CCD, which has a pixel scale of 0″.47. The field of view of the CCD, 16′.3 × 16′.3, encompassed all of NGC 4278 and 4494 and included all but the outermost regions of NGC 4565. Table 1 summarizes the two runs involved. All our narrowband images were 1 hr exposures; our intermediate band off-line images were 9 minute integrations. While NGC 4278 was observed under excellent conditions, the observations of NGC 4494 and NGC 4565 were complicated by periods of poor seeing and occasional thin cirrus. Consequently, the usable data on these latter two galaxies consisted of the best six (of eight) exposures for NGC 4494 and the best three (of six) frames for NGC 4565. Those frames used in the final co-added image are noted in Table 1.

Our PN survey technique was as described in previous papers of the series (see, for example, Jacoby et al. 1989). Each galaxy was imaged in both a narrowband filter transmitting ~30 Å around the [O III] λ5007 emission line (shifted to match the redshift of the galaxy) and through a wider off-band filter transmitting ~300 Å centered near 5275 Å. PN candidates were identified both by blinking the on-band/off-band image pairs and also by selecting positive residuals on "difference" images that were formed by subtracting our scaled continuum images from their on-band counterparts. Although our grand sum images were all built using software that rejects radiation events (the IRAF IMCOMBINE task), each PN candidate was also visually examined to be certain that it exhibited a normal stellar

TABLE 1

OBSERVING LOG

Galaxy	Date	Filter	Seeing	Sky	In Co-added Image?
NGC 4278......	1995 Apr 4	5016/31	1″.4	clear	yes
	1995 Apr 4	5016/31	1.4	clear	yes
	1995 Apr 4	5016/31	1.4	clear	yes
	1995 Apr 5	5016/31	1.2	thin cirrus	yes
	1995 Apr 4	5312/267	1.3	clear	yes
	1995 Apr 4	5312/267	1.2	clear	yes
	1995 Apr 4	5312/267	1.2	clear	yes
	1995 Apr 5	5312/267	1.4	thin cirrus	yes
NGC 4494......	1992 Apr 6	5025/32	2.2	clear	no
	1992 Apr 6	5025/32	1.4	clear	yes
	1992 Apr 6	5025/32	2.1	clear	no
	1992 Apr 7	5025/32	1.6	cirrus	yes
	1992 Apr 7	5025/32	1.3	cirrus	yes
	1992 Apr 7	5025/32	1.2	cirrus	yes
	1992 Apr 7	5025/32	1.0	cirrus	yes
	1992 Apr 7	5025/32	1.1	cirrus	yes
	1992 Apr 6	5290/285	2.0	clear	no
	1992 Apr 6	5290/285	1.9	clear	no
	1992 Apr 6	5290/285	2.0	clear	no
	1992 Apr 7	5290/285	1.1	cirrus	yes
	1992 Apr 7	5290/285	1.2	cirrus	yes
	1992 Apr 7	5290/285	1.2	cirrus	yes
	1992 Apr 7	5290/285	1.2	cirrus	yes
NGC 4565......	1992 Apr 4	5025/32	1.4	cirrus	yes
	1992 Apr 4	5025/32	1.4	cirrus	yes
	1992 Apr 4	5025/32	1.7	cirrus	no
	1992 Apr 5	5025/32	1.4	clear	yes
	1992 Apr 5	5025/32	1.6	cirrus	no
	1992 Apr 6	5025/32	2.2	clear	no
	1992 Apr 7	6619/62	1.9	cirrus	yes
	1992 Apr 4	5312/267	2.1	cirrus	no
	1992 Apr 4	5312/267	2.1	cirrus	no
	1992 Apr 4	5312/267	2.0	cirrus	no
	1992 Apr 4	5312/267	2.0	cirrus	no
	1992 Apr 6	5290/285	1.8	clear	no
	1992 Apr 6	5290/285	1.9	clear	no
	1992 Apr 6	5290/285	2.1	clear	no
	1992 Apr 6	5290/285	2.1	clear	no
	1992 Apr 6	5290/285	1.6	clear	yes
	1992 Apr 6	5290/285	1.6	clear	yes
	1992 Apr 6	5290/285	1.3	clear	yes
	1992 Apr 6	5290/285	1.6	clear	yes

point spread function (PSF) rather than the atypical pattern associated with "cosmic rays."

For the elliptical galaxies NGC 4278 and NGC 4494, we assumed that contamination of our PN sample by H II regions is unlikely (but see § 5). For the Sb galaxy NGC 4565, however, H II regions are abundantly evident. To minimize the confusion caused by these objects, we applied the following safeguards. First, we rejected any spatially resolved emission source, since PNs at ~10 Mpc are always stellar. Second, we obtained a 1 hr Hα image of NGC 4565 to derive an approximate ratio $R = I(\lambda 5007)/I(H\alpha)$ for each object; bright PNs strongly tend to $R \sim 3$ whereas H II regions normally have $R \leq 1$. Third, we avoided objects within 20″ (~1 kpc) of the plane of this nearly edge-on (inclination ~86°; de Vaucouleurs 1958) galaxy. With these filters applied, we expect that few, if any, interloper H II regions remain in our PN sample. In all, we identified 39 PN candidates in NGC 4278, 183 in NGC 4494, and 35 in NGC 4565.

Equatorial coordinates for all the PNs and several reference stars were derived with the *Hubble Space Telescope* (*HST*) Guide Star catalog to define the coordinate system of each galaxy field. Within each field, the coordinate systems have uncertainties of ~0″.5.

Photometry of the PN candidates was performed relative to field stars on each frame with the DAOPHOT point spread function fitting routines (Stetson 1987) within IRAF. For NGC 4494 and 4565, the magnitudes of the field stars were determined by comparing their large-aperture magnitudes to those of four Stone (1977) spectrophotometric standard stars (BD +25 3941, BD +8 2015, Feige 34, and Kopff 27) taken on the night of UT 1992 April 6. Although this night appeared photometric, the 0.04 mag dispersion in the zero-point solution derived from these standards is somewhat higher than the 0.02 mag generally seen, and suggests that thin clouds may have been present during the observations. NGC 4278's field stars were calibrated in a similar manner with the Stone (1977) and Oke (1974) spectrophotometric standards G191B2B, Feige 34, and BD +33 2642. This latter calibration was performed on two different nights; the difference between the two nights was less than 0.02 mag.

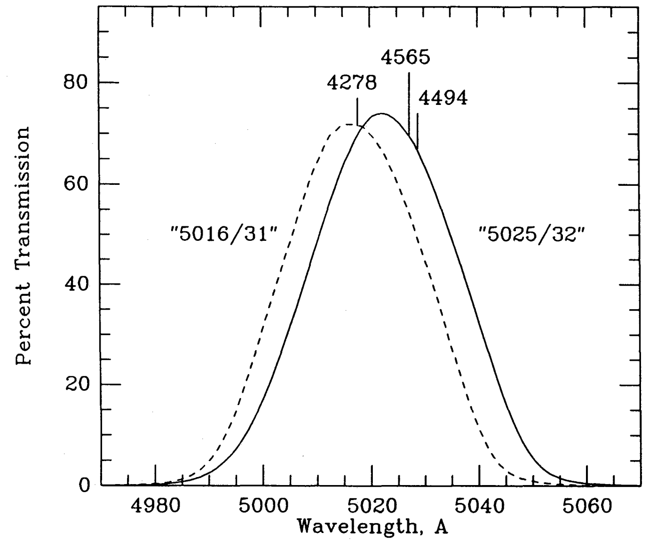

FIG. 1.—Transmission curves for the two on-band filters used in this survey. The dashed line illustrates the filter used for NGC 4278; the solid line defines the filter employed for NGC 4494 and 4565. Both curves are for observations taken in the converging f/2.7 beam of the Kitt Peak 4 m prime focus, and account for the wavelength shift caused by the ambient temperature (10° C for NGC 4278, 8° C for NGC 4494 and 4565). The wavelengths of [O III] λ5007 at the systemic velocities of the galaxies are marked.

For the final step in our reductions, we computed the standard magnitudes for the planetary nebulae using the photometric procedures for emission-line objects described by Jacoby, Quigley, & Africano (1987). The filter transmission curves, corrected for the f/2.7 beam of the telescope and the temperature of the filter at the telescope, are illustrated in Figure 1. The assumed galactic systemic velocities were taken from the Third Reference Catalog of Bright Galaxies (de Vaucouleurs et al. 1991, hereafter RC3), while the envelope velocity dispersions for NGC 4278 and 4494 were estimated from Davies & Birkinshaw (1988) and Jedrzejewski & Schechter (1989). The halo PNs of NGC 4565 were assumed to have a velocity dispersion of ~100 km s^{-1}.

Tables 2–4 list the PN candidates identified in the three galaxies, their epoch 2000 coordinates, and their λ5007-

TABLE 2

NGC 4278 PLANETARY NEBULAE

ID	α(2000)	δ(2000)	R_{iso}(′)	m_{5007}	Notes	ID	α(2000)	δ(2000)	R_{iso}(′)	m_{5007}	Notes
1	12 20 28.94	29 15 49.4	5.7	25.03	Hα	21	12 19 55.18	29 19 38.9	4.5	26.78	S
2	12 20 23.36	29 11 13.5	8.1	25.45	Resolved	22	12 19 49.49	29 16 22.1	4.1	26.83	S
3	12 20 10.95	29 18 15.5	1.7	25.74	S	23	12 20 04.20	29 15 40.2	1.3	26.84	
4	12 20 01.08	29 18 52.0	2.7	25.96	S	24	12 20 04.69	29 15 30.2	1.4	26.91	
5	12 20 22.02	29 15 34.3	4.1	26.01	S	25	12 20 07.38	29 23 49.7	7.7	26.94	S
6	12 20 21.92	29 15 51.9	4.0	26.15	S	26	12 19 50.95	29 15 18.4	3.9	26.94	S
7	12 20 10.36	29 16 52.6	0.9	26.25		27	12 19 59.88	29 15 43.7	1.9	26.97	S
8	12 19 36.61	29 14 59.3	7.3	26.26	S	28	12 20 21.54	29 16 07.4	3.8	26.98	S
9	12 20 26.56	29 19 20.5	5.1	26.35	S	29	12 19 56.60	29 13 53.0	3.7	27.02	S
10	12 20 23.50	29 16 13.2	4.2	26.35	S	30	12 20 02.37	29 15 15.5	1.8	27.05	S
11	12 19 54.71	29 14 20.4	3.6	26.36	S	31	12 19 45.79	29 11 40.9	6.9	27.15	
12	12 20 01.06	29 15 52.2	1.6	26.54	S	32	12 19 59.10	29 18 30.3	2.7	27.17	
13	12 20 18.40	29 17 08.5	2.8	26.59	S	33	12 20 13.53	29 23 08.5	6.8	27.18	
14	12 20 05.01	29 13 42.8	3.3	26.61	S	34	12 20 02.64	29 20 10.4	3.9	27.18	
15	12 20 16.47	29 14 40.3	3.5	26.65	S	35	12 19 34.50	29 16 25.1	7.9	27.19	
16	12 20 03.45	29 17 20.2	1.0	26.66		36	12 20 01.14	29 15 21.7	1.9	27.22	
17	12 20 12.72	29 16 06.6	1.7	26.67	S	37	12 19 59.72	29 15 44.5	1.9	27.30	
18	12 20 07.16	29 13 36.4	3.5	26.68	S	38	12 19 50.24	29 17 56.1	4.3	27.39	
19	12 20 10.46	29 17 48.5	1.3	26.76		39	12 19 56.86	29 14 40.1	3.0	27.67	
20	12 20 09.76	29 18 33.8	1.9	26.78	S						

TABLE 3

NGC 4494 PLANETARY NEBULAE

ID	α(2000)	δ(2000)	$R_{iso}(')$	m_{5007}	Notes	ID	α(2000)	δ(2000)	$R_{iso}(')$	m_{5007}	Notes
1	12 31 23.19	25 46 53.0	0.5	25.68		56	12 31 19.47	25 47 00.5	1.3	26.53	S
2	12 31 25.68	25 46 09.5	0.5	25.90		57	12 31 28.73	25 44 33.9	2.2	26.54	S
3	12 31 21.78	25 47 02.9	0.9	25.99		58	12 31 28.12	25 45 18.4	1.5	26.55	S
4	12 31 21.45	25 46 07.2	0.8	26.01		59	12 31 13.80	25 44 50.4	3.2	26.55	S
5	12 31 22.84	25 45 41.3	0.9	26.06		60	12 31 18.20	25 46 53.0	1.6	26.55	S
6	12 31 25.97	25 46 09.5	0.6	26.13		61	12 31 25.78	25 45 42.2	0.9	26.56	
7	12 31 20.23	25 47 31.4	1.4	26.15	S	62	12 31 20.18	25 47 29.0	1.4	26.56	S
8	12 31 27.03	25 46 02.3	0.9	26.16		63	12 31 18.05	25 44 13.4	2.8	26.57	S
9	12 31 24.08	25 47 41.5	1.2	26.17	S	64	12 31 29.98	25 45 53.0	1.6	26.57	S
10	12 31 29.87	25 45 55.5	1.5	26.17	S	65	12 31 22.18	25 45 48.7	0.8	26.57	
11	12 31 28.97	25 45 33.2	1.5	26.17	S	66	12 31 16.54	25 44 13.8	3.0	26.59	S
12	12 31 15.07	25 47 19.7	2.5	26.19	S	67	12 31 26.56	25 43 36.3	2.9	26.61	S
13	12 31 11.92	25 46 38.3	3.2	26.19	S	68	12 31 22.88	25 45 58.3	0.6	26.61	
14	12 31 16.16	25 46 35.9	2.1	26.21	S	69	12 31 28.55	25 46 59.1	1.3	26.61	S
15	12 31 18.29	25 46 29.4	1.5	26.30	S	70	12 31 21.04	25 47 19.4	1.2	26.62	S
16	12 31 23.08	25 45 55.6	0.6	26.30		71	12 31 23.73	25 45 24.3	1.1	26.62	S
17	12 31 23.04	25 45 51.6	0.7	26.32		72	12 31 32.23	25 45 52.3	2.2	26.63	S
18	12 31 23.37	25 47 14.9	0.8	26.32		73	12 31 23.09	25 45 27.4	1.0	26.63	S
19	12 31 22.94	25 47 11.6	0.8	26.33		74	12 31 35.48	25 46 14.2	2.9	26.63	S
20	12 31 21.65	25 47 09.4	0.9	26.34		75	12 31 20.46	25 46 23.5	1.0	26.64	
21	12 31 27.49	25 47 13.5	1.2	26.35	S	76	12 31 22.57	25 46 50.7	0.6	26.64	
22	12 31 22.96	25 45 44.9	0.8	26.36		77	12 31 26.14	25 47 43.0	1.4	26.64	S
23	12 31 24.65	25 46 58.6	0.5	26.36		78	12 31 28.09	25 46 48.6	1.1	26.64	S
24	12 31 30.07	25 47 13.1	1.7	26.37	S	79	12 31 37.03	25 43 26.1	4.5	26.64	S
25	12 31 27.50	25 47 01.1	1.0	26.37	S	80	12 31 24.15	25 47 45.9	1.3	26.66	S
26	12 31 14.33	25 46 22.7	2.5	26.39	S	81	12 31 28.39	25 43 52.7	2.8	26.66	S
27	12 31 21.90	25 46 57.3	0.8	26.40		82	12 31 28.69	25 46 19.3	1.2	26.67	S
28	12 31 23.47	25 47 33.0	1.1	26.41	S	83	12 31 29.48	25 47 07.3	1.5	26.67	S
29	12 31 15.07	25 45 33.8	2.5	26.41	S	84	12 31 18.12	25 46 02.5	1.6	26.68	S
30	12 31 20.40	25 46 53.4	1.1	26.42	S	85	12 31 25.70	25 47 12.1	0.9	26.69	
31	12 31 27.00	25 45 53.8	0.9	26.42		86	12 31 15.07	25 47 06.1	2.4	26.69	S
32	12 31 19.56	25 47 12.2	1.4	26.43	S	87	12 31 21.97	25 46 48.2	0.7	26.69	
33	12 31 24.55	25 47 54.8	1.5	26.43	S	88	12 31 25.00	25 47 26.1	1.0	26.70	S
34	12 31 22.62	25 45 47.7	0.8	26.43		89	12 31 25.00	25 47 02.2	0.6	26.70	
35	12 31 18.56	25 48 10.5	2.2	26.44	S	90	12 31 18.85	25 43 32.0	3.3	26.71	S
36	12 31 24.99	25 45 10.8	1.3	26.44	S	91	12 31 19.49	25 45 42.5	1.4	26.72	S
37	12 31 24.06	25 47 06.8	0.6	26.44		92	12 31 29.42	25 46 56.1	1.5	26.72	S
38	12 31 22.52	25 46 00.1	0.6	26.45		93	12 31 14.60	25 45 12.7	2.8	26.72	S
39	12 31 23.52	25 45 27.8	1.0	26.45	S	94	12 31 29.08	25 46 32.0	1.3	26.73	S
40	12 31 22.50	25 46 46.1	0.5	26.46		95	12 31 22.31	25 46 42.3	0.6	26.74	
41	12 31 22.56	25 47 48.1	1.4	26.46	S	96	12 31 10.84	25 45 29.7	3.6	26.74	S
42	12 31 21.55	25 46 39.9	0.7	26.47		97	12 31 19.56	25 46 14.2	1.2	26.75	S
43	12 31 30.10	25 46 00.2	1.6	26.48	S	98	12 31 29.15	25 46 33.3	1.3	26.75	S
44	12 31 23.24	25 45 47.7	0.7	26.48		99	12 31 15.30	25 46 58.9	2.3	26.75	S
45	12 31 18.48	25 46 57.0	1.5	26.48	S	100	12 31 19.27	25 42 50.1	3.9	26.76	S
46	12 31 23.33	25 45 08.9	1.3	26.48	S	101	12 31 23.49	25 48 13.9	1.8	26.76	S
47	12 31 19.55	25 46 29.3	1.2	26.49	S	102	12 31 27.78	25 46 44.1	1.0	26.78	S
48	12 31 27.87	25 44 34.8	2.1	26.50	S	103	12 31 30.83	25 46 01.8	1.7	26.78	S
49	12 31 30.36	25 47 03.7	1.7	26.50	S	104	12 31 33.27	25 46 53.4	2.4	26.78	S
50	12 31 17.07	25 45 57.0	1.9	26.50	S	105	12 31 28.66	25 45 05.0	1.8	26.79	S
51	12 31 20.99	25 46 35.5	0.8	26.51		106	12 31 21.70	25 45 39.2	1.0	26.80	S
52	12 31 30.12	25 46 23.9	1.5	26.51	S	107	12 31 27.48	25 45 12.7	1.5	26.80	S
53	12 31 27.59	25 46 30.3	0.9	26.51		108	12 31 26.64	25 45 36.4	1.1	26.81	S
54	12 31 27.27	25 47 08.9	1.1	26.53	S	109	12 31 12.30	25 48 20.5	3.6	26.83	S
55	12 31 22.74	25 46 56.5	0.6	26.53		110	12 31 13.88	25 44 15.4	3.5	26.83	S

magnitudes as defined by Ciardullo et al. (1989b),

$$m_{5007} = -2.5 \log F_{5007} - 13.74 . \qquad (1)$$

The mean errors in the photometric measurements, as reported by the PSF-fitting algorithms of DAOPHOT, are listed in Table 5 as a function of m_{5007}. Table 6 gives the positions of astrometric reference stars.

3. DISTANCES

3.1. *Defining the Statistical Samples*

Plots of the raw PNLFs are shown in Figure 2. The fact that each PNLF begins near a bright limit of $m_{5007} \sim 25.6$ indicates that all three galaxies are crudely at the same distance. The turndown at magnitudes fainter than $m_{5007} \gtrsim 26.7$ is due to incompleteness and confirms that the observing conditions for NGC 4278 were substantially better than those for NGC 4494 or 4565.

In order to form a statistical sample of PNs in each galaxy, we began by considering the detectability of a planetary nebula versus galactic radius. The signal-to-noise ratio of a PN measurement depends both on the magnitude of the object and on the brightness of the background galaxy. Hence, the threshold for PN detection decreases as one searches closer in toward the galaxy nucleus. To avoid variations in our detection limits, we formed our statistical samples using only those objects projected in regions where the surface brightness of the underlying galaxy is less than that of the background sky. Theoretical and empirical tests have shown that when samples are defined in this way, the limiting magnitude for completeness is very nearly the place where the raw PNLF begins to drop (Ciardullo et al. 1987;

TABLE 3—*Continued*

ID	α(2000)	δ(2000)	R_{iso}(′)	m_{5007}	Notes
111	12 31 20.08	25 48 29.8	2.3	26.83	S
112	12 31 29.80	25 45 42.1	1.6	26.83	S
113	12 31 18.26	25 44 40.5	2.4	26.84	S
114	12 31 22.87	25 45 14.9	1.3	26.85	S
115	12 31 37.04	25 49 00.4	4.2	26.86	S
116	12 31 23.24	25 44 45.6	1.7	26.88	S
117	12 31 35.19	25 46 36.5	2.9	26.89	S
118	12 31 31.29	25 47 33.6	2.2	26.91	S
119	12 31 16.26	25 44 49.0	2.6	26.92	S
120	12 31 20.66	25 46 16.9	0.9	26.92	
121	12 31 24.95	25 47 23.3	0.9	26.93	
122	12 31 19.69	25 44 15.0	2.5	26.93	S
123	12 31 30.90	25 44 04.1	2.9	26.93	S
124	12 31 31.03	25 47 47.5	2.2	26.94	S
125	12 31 20.85	25 45 39.7	1.2	26.95	S
126	12 31 30.88	25 45 46.3	1.8	26.95	S
127	12 31 22.19	25 45 32.7	1.1	26.95	S
128	12 31 20.80	25 46 20.5	0.9	26.96	
129	12 31 27.52	25 46 48.3	0.9	26.96	
130	12 31 24.52	25 47 38.4	1.2	26.97	S
131	12 31 17.30	25 44 05.4	3.0	26.97	S
132	12 31 21.72	25 45 28.7	1.2	26.98	S
133	12 31 24.08	25 47 09.8	0.7	26.98	
134	12 31 18.92	25 45 09.8	1.9	26.98	S
135	12 31 30.13	25 44 52.2	2.2	26.98	S
136	12 31 33.25	25 45 16.1	2.6	26.98	S
137	12 31 23.65	25 48 08.6	1.7	26.98	S
138	12 31 16.05	25 45 15.7	2.4	26.98	S
139	12 31 24.04	25 48 19.1	1.9	26.98	S
140	12 31 21.34	25 47 54.7	1.6	27.00	S
141	12 31 23.98	25 47 11.3	0.7	27.02	
142	12 31 36.48	25 45 19.5	3.4	27.02	
143	12 31 19.04	25 45 35.1	1.6	27.02	
144	12 31 19.20	25 45 28.8	1.6	27.02	
145	12 31 24.16	25 44 52.4	1.6	27.03	
146	12 31 33.45	25 49 14.5	3.7	27.03	
147	12 31 27.28	25 48 23.3	2.1	27.04	
148	12 31 19.52	25 47 05.3	1.3	27.04	
149	12 31 25.54	25 47 20.3	0.9	27.04	
150	12 31 32.64	25 46 07.5	2.2	27.05	
151	12 31 23.28	25 47 25.9	1.0	27.06	
152	12 31 37.37	25 47 29.5	3.6	27.06	
153	12 31 26.92	25 45 27.0	1.2	27.08	
154	12 31 23.78	25 47 36.2	1.1	27.10	
155	12 31 21.00	25 47 50.9	1.6	27.10	
156	12 31 20.72	25 47 25.1	1.3	27.11	
157	12 31 30.95	25 44 01.0	3.0	27.12	
158	12 31 27.62	25 44 51.0	1.8	27.12	
159	12 31 35.32	25 47 53.4	3.3	27.12	
160	12 31 32.59	25 45 50.4	2.2	27.14	
161	12 31 26.36	25 45 35.9	1.0	27.15	
162	12 31 34.62	25 44 54.2	3.1	27.17	
163	12 31 18.53	25 44 10.6	2.8	27.17	
164	12 31 25.23	25 47 21.9	0.9	27.18	
165	12 31 18.01	25 47 02.3	1.6	27.18	
166	12 31 18.69	25 45 25.4	1.8	27.19	
167	12 31 24.94	25 44 46.1	1.7	27.20	
168	12 31 18.09	25 46 11.1	1.6	27.20	
169	12 31 28.48	25 46 19.3	1.1	27.21	
170	12 31 14.12	25 43 39.9	3.9	27.21	
171	12 31 18.17	25 47 03.1	1.6	27.22	
172	12 31 34.55	25 47 46.5	3.0	27.23	
173	12 31 32.34	25 43 30.9	3.6	27.23	
174	12 31 36.70	25 46 32.9	3.3	27.24	
175	12 31 27.27	25 47 32.4	1.4	27.27	
176	12 31 19.25	25 45 33.6	1.6	27.27	
177	12 31 35.74	25 47 56.3	3.4	27.28	
178	12 31 25.89	25 43 35.3	2.9	27.34	
179	12 31 36.72	25 45 31.1	3.4	27.36	
180	12 31 22.00	25 47 17.4	1.0	27.38	
181	12 31 32.52	25 45 46.0	2.2	27.59	
182	12 31 18.82	25 45 24.2	1.8	27.65	
183	12 31 19.26	25 45 40.0	1.5	27.69	

Ciardullo, Jacoby, & Ford 1989a; Hui et al. 1993). Moreover, small (~0.1 mag) errors in the definition of this limit have little or no effect on the derived distances. Thus, for NGC 4278, our statistical sample included only those PNs brighter than $m_{5007} = 27.1$ that are projected outside the galaxy's isophote at 1′.5 (semimajor axis); for NGC 4494, the sample consisted of PNs with $m_{5007} < 27.0$ and isophotal radii $R_{iso} > 1'.0$. For the spiral galaxy NGC 4565, our sample of objects consisted of PNs projected more than 20″ from the galactic plane and with $m_{5007} < 26.5$. This information is summarized in Table 7. The isophotal radius or z distance of each planetary nebulae is included in Tables 2–4. Those PNs that are part of the statistical samples are marked with an "S."

Before deriving distances, one additional remark should be made concerning the PN candidates of NGC 4278. An inspection of Figure 2 shows that, while the PNLFs of NGC 4494 and 4565 exhibit a sharp cutoff at the bright end of the

TABLE 4

NGC 4565 PLANETARY NEBULAE

ID	α(2000)	δ(2000)	z(″)	m_{5007}	Notes
1	12 36 16.52	25 59 32.4	28	25.76	S
2	12 36 26.38	25 57 28.5	20	25.86	S
3	12 36 21.62	25 58 23.5	27	25.91	S
4	12 36 20.04	25 58 22.9	43	25.91	S
5	12 36 21.81	25 58 14.1	32	26.00	S
6	12 36 28.64	25 58 30.0	45	26.09	S
7	12 36 29.56	25 57 49.4	25	26.16	S
8	12 36 13.49	25 59 59.8	37	26.17	S
9	12 36 09.00	26 03 04.0	49	26.19	S
10	12 36 15.75	25 59 21.9	43	26.20	S
11	12 36 36.33	25 56 01.6	15	26.26	
12	12 36 12.88	26 00 25.6	25	26.28	S
13	12 36 31.60	25 57 20.4	25	26.29	S
14	12 36 27.62	25 56 12.1	61	26.30	S
15	12 36 27.41	25 56 20.2	58	26.31	S
16	12 36 35.26	25 57 14.4	56	26.32	S
17	12 36 13.52	26 02 06.6	52	26.42	S
18	12 36 04.65	26 02 22.7	22	26.44	S
19	12 36 16.77	25 58 57.8	50	26.47	S
20	12 36 14.85	26 01 20.0	32	26.49	S
21	12 36 15.21	26 01 11.4	29	26.58	
22	12 36 29.59	25 56 35.3	26	26.58	
23	12 36 25.97	25 58 44.8	30	26.59	
24	12 36 24.00	25 57 50.7	27	26.63	
25	12 36 14.53	25 59 55.8	31	26.71	
26	12 36 25.05	25 59 37.1	58	26.71	
27	12 36 41.03	25 55 18.1	29	26.72	
28	12 36 05.39	26 02 14.7	20	26.76	
29	12 36 30.41	25 56 28.0	23	26.82	
30	12 36 30.61	25 56 31.7	19	26.99	
31	12 36 18.55	25 57 52.8	78	27.02	
32	12 36 10.14	26 01 05.7	23	27.19	
33	12 36 12.07	26 00 17.1	39	27.22	
34	12 36 07.03	25 58 24.5	166	27.41	
35	12 36 08.86	25 58 50.0	131	27.77	

TABLE 5

PLANETARY NEBULA PHOTOMETRIC ERROR VERSUS MAGNITUDE

Magnitude	NGC 4278	NGC 4494	NGC 4565
25.00	0.03	...	...
25.25	...	...	...
25.50	0.05	...	...
25.75	0.06	...	0.07
26.00	0.07	...	0.07
26.25	0.08	0.10	0.08
26.50	0.09	0.11	0.10
26.75	0.10	0.12	0.12
27.00	0.12	0.14	0.16
27.25	0.15	0.16	0.19
27.50	0.18	0.20	0.22

luminosity function, NGC 4278's luminosity function also has a conspicuous overluminous tail. The brightest of NGC 4278's [O III] λ5007 sources is nearly 1 mag brighter than the apparent PNLF cutoff; the second brightest object is ~0.5 mag brighter than the break. Remarkably, both sources are, in reality, intracluster in origin: PN candidate 1 is projected more than $10r_e$ from the galaxy's nucleus, while candidate 2 is almost $15r_e$ from the galactic center, where r_e is the effective radius of the galaxy.

Strictly speaking, the two "overluminous" objects listed in Table 4 are not planetary nebula candidates. A deep Hα image taken during the course of a nova survey of NGC 4278 (Shafter, Ciardullo, & Pritchet 1996) reveals that the brightest [O III] λ5007 source is even brighter in Hα. This

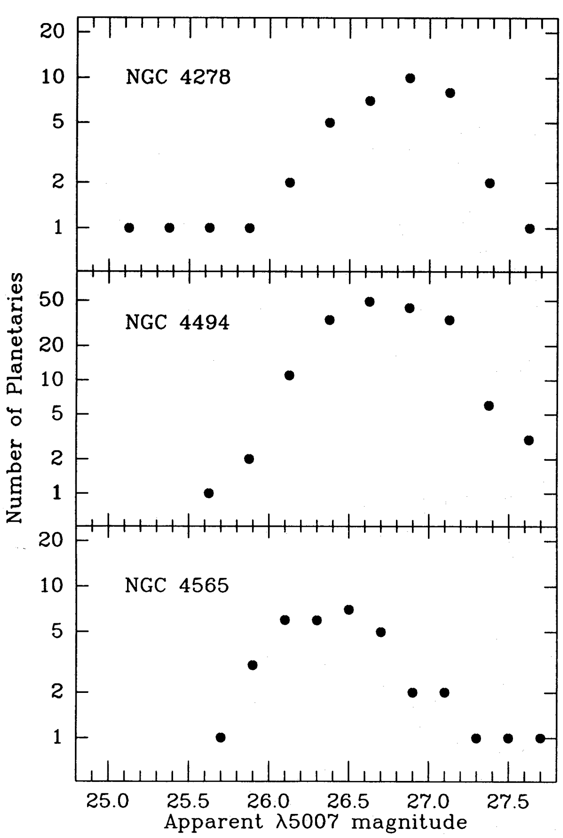

FIG. 2.—Raw PNLFs of NGC 4278, 4494, and 4565. Magnitudes are defined as in Ciardullo et al. (1989b) and eq. (1). Although the PNLFs are generally similar in form, it is apparent that the PNLF for NGC 4565 becomes incomplete at a significantly brighter limit than for NGC 4278 or 4494. Also apparent are the two overluminous objects of NGC 4278: although neither is a true PN, they are included here for completeness.

TABLE 6

ASTROMETRIC REFERENCE STARS

Galaxy	ID	α(2000)	δ(2000)
NGC 4278	a	12 19 53.64	29 13 18.2
	b	12 20 11.13	29 13 54.3
	c	12 20 23.53	29 15 55.4
	d	12 19 48.10	29 15 09.0
	e	12 19 59.68	29 21 55.0
	f	12 20 11.97	29 12 39.5
	g	12 20 27.16	29 19 08.5
	h	12 20 10.06	29 22 37.0
	i	12 19 35.59	29 22 34.3
	j	12 20 38.61	29 20 05.0
	k	12 20 44.08	29 20 01.6
NGC 4494	a	12 31 17.01	25 46 19.2
	b	12 31 16.78	25 47 12.0
	c	12 31 10.94	25 43 12.3
	d	12 31 05.68	25 50 43.0
	e	12 31 03.39	25 50 42.9
	f	12 31 37.12	25 40 10.1
	g	12 31 43.20	25 39 20.2
	h	12 31 54.53	25 50 56.2
	i	12 31 55.23	25 38 34.4
	j	12 31 09.31	25 48 45.5
	k	12 31 15.94	25 47 01.9
	l	12 31 11.74	25 43 54.4
NGC 4565	a	12 36 44.32	25 55 49.4
	b	12 36 01.53	26 01 13.3
	c	12 35 59.49	26 00 44.6
	d	12 36 16.82	26 03 54.3
	e	12 36 24.76	26 05 39.4
	f	12 36 32.68	26 06 14.0
	g	12 35 56.55	26 03 07.9
	h	12 36 18.87	25 52 07.3
	i	12 36 13.25	25 51 45.6
	j	12 36 04.62	25 54 25.3
	k	12 36 47.93	25 58 27.5
	l	12 35 50.98	25 57 16.3
	m	12 35 54.09	25 57 03.9
	n	12 35 55.57	25 58 07.9
	o	12 36 08.61	25 58 27.1
	p	12 36 12.22	25 59 52.0
	q	12 36 03.48	26 04 16.5
	r	12 36 37.10	25 57 43.2
	s	12 36 38.64	26 04 45.2
	t	12 36 10.09	25 56 57.4
	u	12 36 08.46	25 56 21.9
	v	12 36 46.40	26 00 34.4
	w	12 36 44.49	26 05 17.6

suggests that the candidate is either a supernova remnant or an H II region and should be excluded from the analysis. Similarly, although PN candidate 2 is invisible in Hα and thus has the excitation of a planetary nebula, a careful inspection of its image shows that it is marginally resolved with an intrinsic FWHM of ~0ʺ.6. Hence, it too should be omitted from our sample. Both objects are included in our PN table for purposes of completeness: had the galaxy been further away, or not been surveyed for novae, both would have been classified as "overluminous PN candidates." We will return to these objects in § 5.

3.2. *Maximum-Likelihood Solutions*

The PNLF distances to NGC 4278, 4494, and 4565 and their formal uncertainties were calculated by convolving the empirical function (Ciardullo et al. 1989b)

$$N(M) \propto e^{0.307M}[1 - e^{3(M^* - M)}] , \qquad (2)$$

with the photometric errors of Table 5 and fitting the resultant curve to the observed PNLFs via the method of

TABLE 7

SUMMARY FOR COMA I GALAXIES

Parameter	NGC 4278	NGC 4494	NGC 4565
Galaxy Type (RSA)	E1	E1	Sb
BT (RC3)	11.09	10.71	10.42
Systemic Velocity (km s^{-1})	649	1324	1227
A_B (B&H)	0.10	0.06	0.04
Separation from NGC 4565	4°9	1°1	...
V(sampled)	11.2	11.0	10.8
PN completeness limit	27.1	27.0	26.5
Location of completeness	R(iso) > 90″	R(iso) > 60″	z > 20″
Number of PN found	39	183	35
Number of PN in sample	23	101	17
Best-fitting $(m - M)_0$	$30.04^{+0.08}_{-0.16}$	$30.54^{+0.04}_{-0.05}$	$30.12^{+0.07}_{-0.13}$
$\alpha_{2.5}$	$10.5^{+2.4}_{-2.0}$	$49.3^{+5.5}_{-4.8}$	$11.7^{+3.5}_{-2.6}$

maximum likelihood (Ciardullo et al. 1989b). As in previous studies, we adopted $M^* = -4.48$, based on a distance to M31 of 710 kpc (Welch et al. 1986), a foreground reddening of $E(B-V) = 0.11$ (McClure & Racine 1969), and a Seaton (1979) reddening curve. With more recent values for M31's distance (770 kpc; Freedman & Madore 1990) and reddening [$E(B-V) = 0.08$; Burstein & Heiles 1984], the distances reported here would increase by $\sim$3%. All our Coma I distances have assumed the foreground extinction values (see Table 7) of Burstein & Heiles (1984).

The maximum-likelihood fits to the observed statistical PNLFs are summarized in Table 7 and shown in Figure 3.

Figure 4 displays the uncertainty of each solution via probability contours. Note that the ordinate of Figure 4 is $\alpha_{2.5}$, the number of PNs within 2.5 mag of M^* normalized to galactic bolometric luminosity. The luminosity normalization of NGC 4278 is based on the surface photometry of Peletier et al. (1990); the normalizations for NGC 4494 and 4565 are derived from B and V CCD photometry performed with the Kitt Peak 0.9 m telescope. Bolometric corrections for NGC 4278 and 4494 were estimated by combining the ultraviolet observations of Burstein et al.

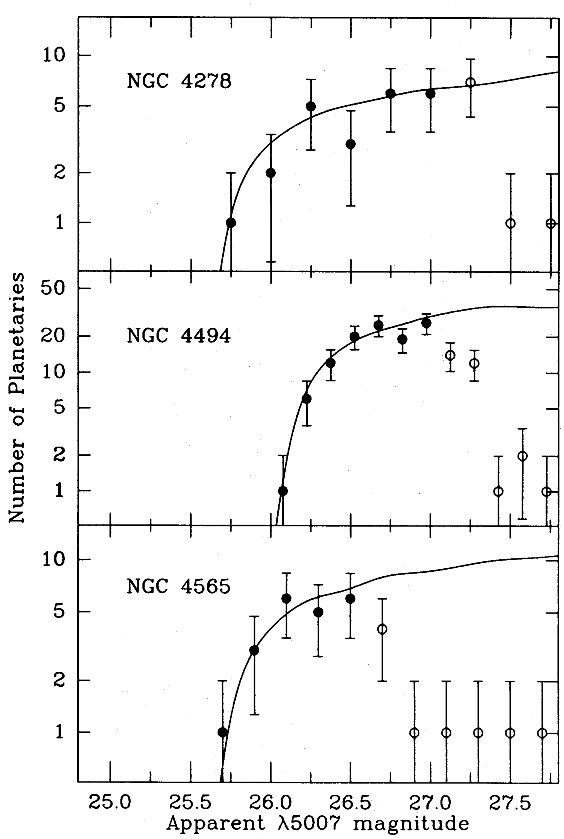

FIG. 3.—PNLFs for NGC 4278, 4494, and 4565 as defined by those PNs in the homogeneously complete sample (*solid points*). Open circles indicate those objects fainter than the completeness limit. Objects 1 and 2 in Table 2 were omitted from this plot because they are not PNs. The solid lines represent the empirical PNLF of eq. (1) convolved with the mean photometric error vs. magnitude relation and translated to the most likely distance modulus for each galaxy.

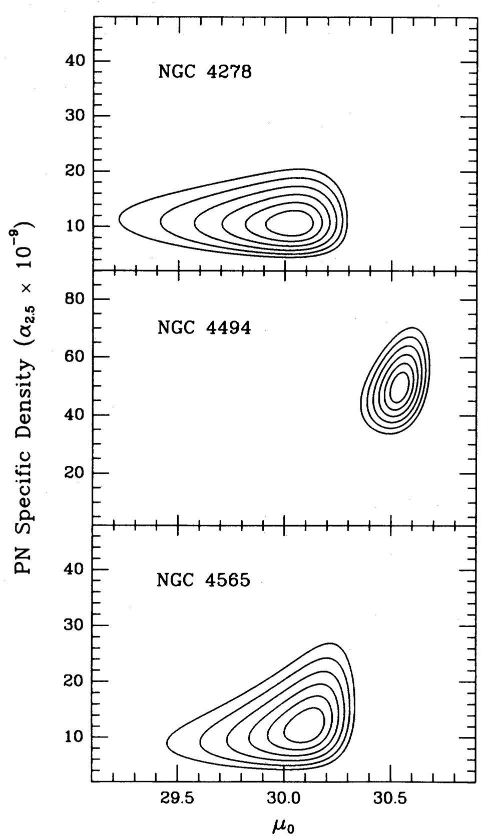

FIG. 4.—Maximum-likelihood contours for NGC 4278, 4494, and 4565 derived from fitting the empirical PNLF (convolved with the photometric error function) to complete samples of PNs in each galaxy. The abscissa is the true distance modulus; the ordinate is the number of PNs within 2.5 mag of the bright end magnitude cutoff, normalized to the amount of bolometric luminosity surveyed. The probability contours are drawn at 0.5 σ intervals. Due to the difficulty in estimating the luminosity and bolometric correction applicable to NGC 4565's halo, the vertical scale for this galaxy is somewhat uncertain.

(1988) with the infrared and optical colors given by Johnson (1966), Frogel et al. (1978), and RC3. The bolometric correction for NGC 4565's halo is an estimate based on the observed $B-V$ color. Note that although the amount of luminosity sampled in NGC 4278 and 4494 is similar, the latter galaxy has a factor of 10 more planetaries in the top $\sim$0.9 mag of its PNLF. This is a result of fundamental differences between the two stellar populations: NGC 4278 has a significant excess of emission in the *IUE* bandpass ($m_{1550} - V = 2.88$), while the UV upturn in NGC 4494 is very mild ($m_{1550} - V = 3.77$; Burstein et al. 1988). The anticorrelation between UV excess and $\alpha_{2.5}$ seen in the two galaxies adds support to the suggestion by Ciardullo, Jacoby, & Harris (1991) and Ferguson & Davidsen (1993) that the ultraviolet flux emitted by old stellar populations comes from stars whose asymptotic branch evolution has been prematurely aborted (Greggio & Renzini 1990; Dorman, Rood, & O'Connell 1993). Similar correlations between galaxy properties ($B-V$, luminosity) and PNs production rates were first noted by Peimbert (1990). These topics will be discussed in detail in a separate paper (Ciardullo, Jacoby, & Feldmeier 1996).

3.3. *Uncertainties*

The uncertainties implied by the contours of Figure 4 are only those internal to the fitting procedure. To compute the total error budget, these uncertainties must be combined with those associated with photometric zero points, the filter response curves, and the Galactic foreground extinctions. (The latter come from Burstein & Heiles 1984.) In addition, two systematic errors, which affect all PNLF measurements the same way, arise from the uncertain definition of the empirical PNLF, and, of course, the distance to the calibration galaxy, M31. These errors are summarized in Table 8.

4. DEPTH OF THE COMA I GROUP

The primary motivation of this study was to assess the reliability of the PNLF method across Hubble types. Our PNLF distances to the three members of the group, NGC 4278, 4494, and 4565, are $10.2^{+0.5}_{-0.8}$, $12.8^{+0.5}_{-0.5}$, and $10.5^{+0.5}_{-0.7}$ Mpc. (Here, we have omitted the possible systematic contribution to the errors.) A comparison of these distances suggests that there is indeed a small, but significant, difference between the distance to the large elliptical NGC 4494 and that of the other two galaxies. Either NGC 4278 and 4565 are $\sim$2 Mpc in front of NGC 4494, or the PNLF distance method is affected by stellar population or sample size.

To test the plausibility of these two alternatives, we plot in Figure 5 the positions of the three galaxies based on distances derived from the PNLF, GCLF, and SBF techniques. These are summarized in Table 9. All three methods agree that the distance to NGC 4565 is $\sim$10 Mpc, but, more importantly, each method finds that NGC 4494 is in the background. According to the SBF method, NGC 4494 and 4565 are separated by 4.6 ± 2.1 Mpc (Simard & Pritchet 1994), the GCLF technique gives a separation of 4.4 ± 3.3 Mpc (Fleming et al. 1995), and the PNLF measurements imply a separation of 2.3 ± 0.8 Mpc. Since all three methods are strikingly different in detail, it is extremely unlikely that the error estimates of the techniques are correlated. This being the case, and if the error bars are accurate, there is less than a 0.1% chance that the two galaxies are members of the same $\sim$1 Mpc size cluster.

Simard & Pritchet (1994) and Fleming et al. (1995) note the fact that the galaxies of Coma I fall near the "triple-value ambiguity" of Virgocentric infall models (see, e.g., Tonry & Davis 1981; Tully & Shaya 1984). Here, the Hubble flow in the direction of Coma I, which is 13° from Virgo, is complicated by Virgo's gravitational attraction. According to the infall model, galaxies having similar radial velocities (1259 km s^{-1} for NGC 4494 and 1171 km s^{-1} for NGC 4565, corrected to the centroid of the Local Group) can be located at distances of $\sim$10–11, $\sim$14–15, or $\sim$21–24 Mpc, depending on the choices for the Virgo distance and Hubble Constant. The PNLF distance measurements to NGC 4565 and 4494 are consistent with those models.

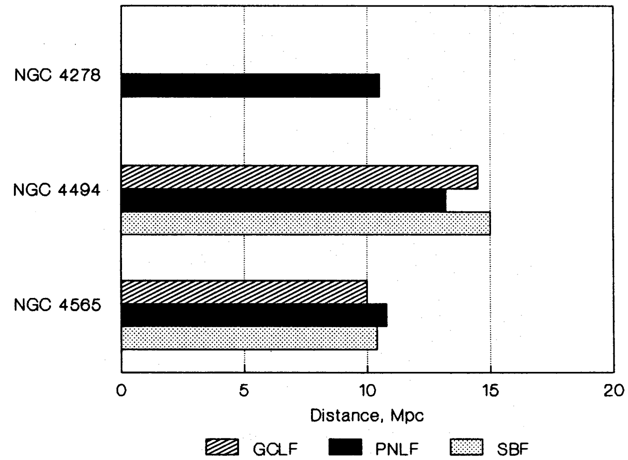

FIG. 5.—Graphical representation of the distances in Table 9, but the PNLF distances have been increased by 3% to place them on the same M31 zero-point system as the other methods. It is clear that NGC 4278 and 4565 have similar distances as measured by their PNLFs, but all three methods place NGC 4494 further away. Given the quoted errors in the methods, it is very likely that NGC 4565 and 4494 are not members of the same $\sim$1 Mpc size cluster.

TABLE 8

SUMMARY OF DISTANCE MODULUS UNCERTAINTIES

Source	NGC 4278	NGC 4494	NGC 4565
Maximum-likelihood fit	$^{+0.08}_{-0.16}$	$^{+0.04}_{-0.05}$	$^{+0.07}_{-0.13}$
Photometric zero point	0.02	0.04	0.04
Filter response	0.04	0.04	0.04
Foreground extinction	0.05	0.05	0.05
Total random error	$^{+0.10}_{-0.17}$	$^{+0.09}_{-0.09}$	$^{+0.10}_{-0.15}$
PNLF definition	0.05	0.05	0.05
M31 distance	0.10	0.10	0.10
Total error (random + systematic)	$^{+0.15}_{-0.21}$	$^{+0.14}_{-0.14}$	$^{+0.15}_{-0.19}$

TABLE 9

COMPARISON OF DISTANCES TO COMA I GALAXIES

Galaxy	GCLF[a]	SBF[b]	PNLF[c]
NGC 4278......	...	...	$10.2^{+0.7}_{-1.0}$
NGC 4494......	14.5 ± 2.7	15.0 ± 1.9	$12.8^{+0.9}_{-0.9}$
NGC 4565......	10.0 ± 1.5	10.4 ± 0.5	$10.5^{+0.8}_{-1.0}$

a Fleming et al. 1995.
b Simard & Pritchet 1994.
c This paper assumed the M31 distance and reddening of 710 kpc and $E(B-V) = 0.11$, respectively; distances increase by 3% when adopting more recent parameters.

Moreover, the fact that the three methods considered here all produce similar results enhances the arguments of Jacoby et al. (1992), Ciardullo, Jacoby, & Tonry (1993), and Jacoby (1995) that most distance indicators yield completely consistent results. Recent PNLF and *HST* Cepheid distances for M101, for example, yield nearly identical values. Feldmeier, Ciardullo, & Jacoby (1996) obtained 7.7 ± 0.5 Mpc using the PNLF, while Kelson et al. (1994) found 7.5 ± 0.7 Mpc with Cepheids. Previous direct PNLF–Cepheid comparisons in M81, NGC 5253, and NGC 300 also yielded excellent agreement (see Soffner et al. 1996). Similarly, Tanvir et al. (1995) derived an *HST* Cepheid distance to M96 of 11.6 ± 0.8 Mpc. This agrees well with the PNLF distance of 10.4 ± 1.3 Mpc to NGC 3377, NGC 3384, and NGC 3379 (values from Ciardullo et al. 1989a, but corrected to the modern M31 distance and reddening), the companion early-type galaxies to M96 in the Leo group.

5. OVERLUMINOUS [O III] OBJECTS AND THE PNLF

As mentioned above, the PNLF of NGC 4278 is somewhat confused by the presence of "overluminous" objects—that is, objects with an [O III] λ5007-magnitude substantially brighter than m^*. (Here, we define "substantially" as more than 0.2 mag more luminous than m^*; normal PNs may occasionally be recorded as being slightly overluminous due to random photometric error.) We were able to exclude these objects on the basis of their Hα emission and angular extent. However, this information is not always available; had NGC 4278 been at the distance of Virgo, PN 2 would have been included in the complete sample. Similarly, without an Hα image, PN 1 would also have been included. Moreover, the existence of this tail would have called into question the nature of PN 3, which is ~0.2 mag brighter than the next brightest object.

Table 10 lists all the overluminous [O III] λ5007 sources discovered to date, along with their parent galaxies and properties. To be included in the list, an object must have an [O III] λ5007-magnitude more than 0.2 mag brighter that m^* and be indistinguishable from a PN in 1."2 seeing at the distance of Virgo.

5.1. *What Are the Overluminous Sources?*

In order to deal with the problem of overluminous [O III] λ5007 in a PN sample, we must first have some idea as to their origin. There are many possibilities.

H II *regions.*—In some sense, the simplest explanation for the overluminous [O III] λ5007 sources is compact H II regions. At distances of ≳10 Mpc, typical ground-based cameras with 1″ seeing cannot resolve objects smaller than ~30 pc; thus, smaller objects can appear stellar and be identified as planetary nebulae. In 0."8 seeing, Ciardullo et al. (1991) resolved one overluminous object in NGC 1023. Also, PN 2 in NGC 4278 is marginally resolved in 1."3 seeing with an implied linear size of ~30 pc. These objects cannot be PNs, since bright planetaries are never larger than ~1 pc. They can, however, be compact H II regions, which have diameters down to ~10 pc (Kennicutt 1984). While we generally do not expect to see H II regions in elliptical galaxies, some early-type systems, and NGC 4278 in particular, often host pockets of ionized gas. Figure 6 (Plate 1) illustrates that NGC 4278 is an interesting example: after subtracting the continuum image from the [O III] image, an extensive pattern similar to a barred spiral galaxy is revealed.

While we cannot rule out H II regions as being responsible for the overluminous sources, there are several problems with this interpretation. First, although many of the host galaxies in Table 10 are known to contain gas and/or dust, evidence for star formation in them is generally absent. We thus are faced with the question of why the host galaxies are creating compact H II regions, but not larger, more typical ones. Second, although the sample of overluminous PNs is small, the tendency is for these objects to be located at large galactic radii. Under most scenarios, star formation should occur closer to the galactic centers, where the density is higher and the gas is more easily shocked. Finally, the excitation of at least some of these bright sources is much higher than that of a typical H II region. The ratio of Hα to [O III] in NGC 4486's overluminous PNs is ≲0.5, and PN candidate 2 in NGC 4278 was undetectable in a 1 hr Hα image taken with the Kitt Peak 4 m telescope.

TABLE 10

SUMMARY OF λ5007 OVERLUMINOUS SOURCES

Galaxy	ID	$M^* - M_{5007}$	Nr PN	Comments
NGC 1023......	...	0.5	110	Resolved in 0."8 seeing; gas-rich galaxy
NGC 4278......	1	0.6	39	Stellar in 1."3 seeing; $I(H\alpha)/I(\lambda5007) \gtrsim 1$; gas-rich galaxy
	2	0.2	...	Resolved in 1."3 seeing
NGC 4382......	1	1.1	102	Stellar in 1."0 seeing; blue S0 galaxy
NGC 4406......	1	1.0	141	Stellar in 1."1 seeing
	2	0.3	...	Resolved in 1."1 seeing
	3	0.2	...	Stellar in 1."1 seeing
NGC 4374......	1	0.3	102	Stellar in 1."1 seeing
	2	0.2	...	Stellar in 1."1 seeing
	3	0.2	...	Resolved in 1."1 seeing
NGC 4486......	1	0.8	340	Stellar in 0."7 seeing; $I(H\alpha)/I(\lambda5007) \lesssim 0.5$; single narrow line

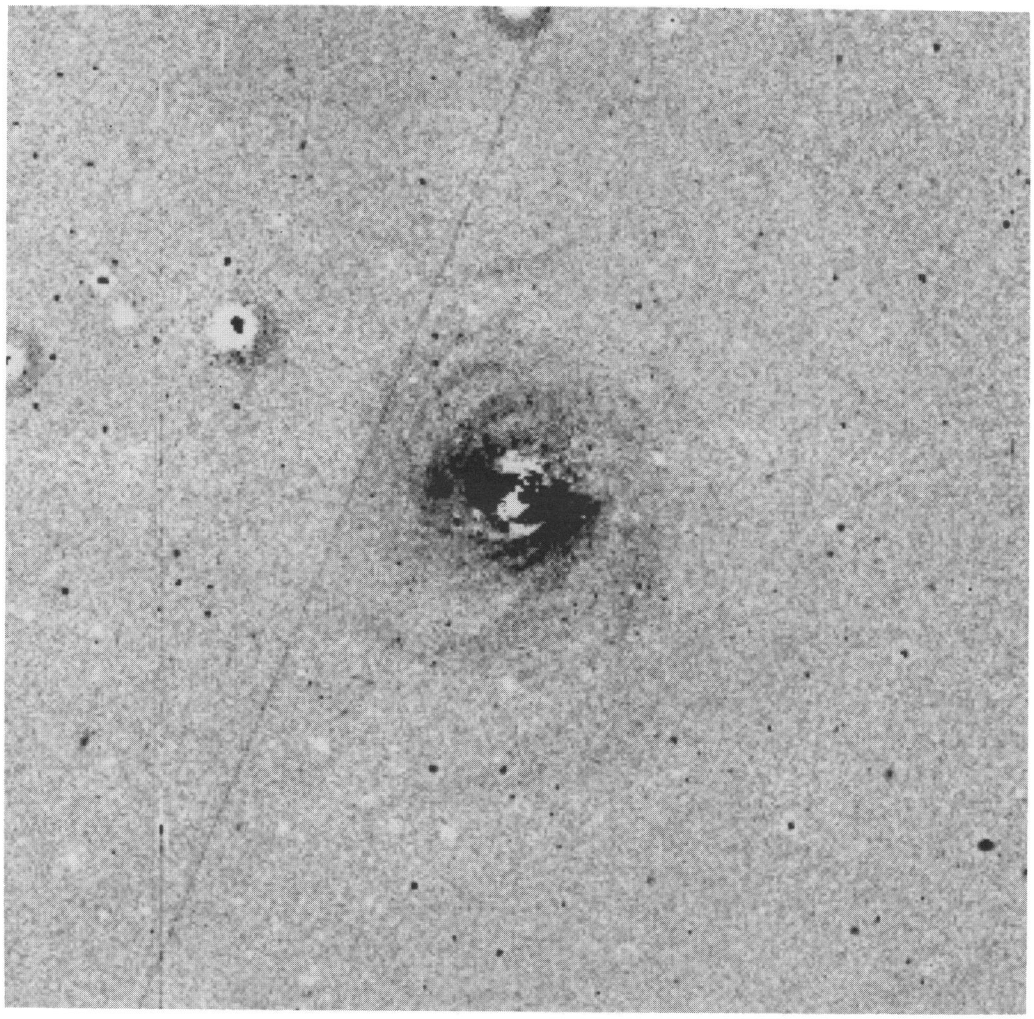

FIG. 6.—Central 11′ × 11′ of the [O III] difference image of the elliptical galaxy NGC 4278. North is displayed up and east is to the left. Although classified as an E1 galaxy, NGC 4278 has a small amount of ionized gas distributed in a barred spiral pattern. Filaments of the gas extend to the edge of the figure, well beyond the usual optical image; one filament apparently passes very close to the small E0 galaxy NGC 4283, which appears as a strong negative (white) residual to the northeast of NGC 4278. There is no evidence for a physical association, otherwise, and NGC 4283 has a velocity ~500 km s^{-1} higher than NGC 4278. Raimond et al. (1981) suggested that a central bar might be present to explain the regular disklike kinematics of an H I cloud that envelopes NGC 4278. They also noted a central hole in the H I emission, which we suggest may be due to the gas being ionized, and they hypothesized that the source of the gas could be from a cannibalized gas-rich dwarf. This [O III] image supports those ideas. The diagonal streak running from due north to the southeast is a satellite trail.

JACOBY, CIARDULLO, & HARRIS (see 462, 9)

Supernova remnants.—Type Ia supernovae occur in early-type galaxies, though at a lower rate than in late-type galaxies (van den Bergh & McClure 1994; van den Bergh & Tammann 1991). In fact, of the six galaxies listed in Table 10, three (NGC 4374, 4382, and 4486) have hosted supernovae in this century alone. However, none of these supernovae was detected in [O III] λ5007 (Jacoby, Ciardullo, & Ford 1990), nor were 1980N and 1981D detected in the planetary nebula survey of NGC 1316 (McMillan, Ciardullo, & Jacoby 1993). This is consistent with the hypothesis presented in Jacoby et al. (1990) that supernovae will be difficult to detect when the interstellar medium in a galaxy is sparse: without a confining medium, the supernova shell will quickly expand to an undetectable low-density, low surface brightness state. It may be significant, however, that NGC 4278 is embedded in a disk of atomic hydrogen that extends $\sim 9 r_e$ into the galaxy's halo (Raimond et al. 1981; Burstein, Krumm, & Salpeter 1987; Lees 1992). Thus, the overluminous objects detected in this galaxy may indeed be the confined remnants of recent supernovae. This is especially true of NGC 4278 PN 1, which is bright in Hα as well as [O III]. Future imaging in [S II] would help discriminate supernova remnants from H II regions.

Wolf-Rayet nebulae: The strong winds and UV emission from Wolf-Rayet stars can interact with their surrounding interstellar medium to create ring nebulae that are similar to planetary nebulae (Chu 1993). Even in the Milky Way, the two can be extremely difficult to distinguish: the nebula M1 − 67 (Minkowski 1946), for example, was classified as a planetary by Bertola (1964) but has since been reclassified as a Wolf-Rayet nebula by Cohen & Barlow (1975), put back in the planetary nebula category by van der Hucht et al. (1985), and returned yet again to Wolf-Rayet status by Esteban et al. (1991) and Crawford & Barlow (1991). Unlike the central stars of PNs, Wolf-Rayet stars can have very high masses (10–50 $M_\odot$; Massey 1981) and luminosities; hence, their nebulae can have the extreme luminosity of an overluminous [O III] source. However, since the Wolf-Rayet phenomenon is short-lived, any association of these objects with the overluminous PNs implies the presence of a substantial population of young, very massive stars in otherwise normal elliptical galaxies.

Supersoft X-ray nebulae: Di Stefano, Paerels, & Rappaport (1995) have modeled the luminosity function expected for nebulae surrounding supersoft X-ray sources. These sources, which may be low-mass X-ray binaries (Cowley et al. 1990) or white dwarfs undergoing steady nuclear burning due to accretion (Rappaport, Di Stefano, & Smith 1994), can extend the PNLF by nearly 1 mag *if* they happen to be surrounded by cold interstellar gas. Unfortunately, the only known example of the class, CAL 83 (Pakull, Ilovaisky, & Chevalier 1985; Remillard, Rappaport, & Macri 1995), is 10 times fainter than M^* and quite extended (∼25 pc). Support for the association of overluminous PNs with supersoft X-ray sources, does come, however, from N67, a bright, normal PN in the Small Magellanic Cloud, which is coincident with the Einstein ultrasoft X-ray source 1E0056.8 − 7154 (Wang 1991; Brown et al. 1994).

PNs from massive progenitors.—By modeling the [O III] λ5007 luminosities expected from ensembles of PNs, Jacoby (1989) found that for a PN to become ∼1 mag brighter than M^*, its central star must be more massive than 0.72 $M_\odot$. From the initial-to-final mass relations of Kwok (1983) and Weidemann (1987), this implies a progenitor mass of $\gtrsim 4$ $M_\odot$ (late B on the main sequence). Since stars of this high mass are extremely short-lived, the probability of catching one near maximum luminosity is very low (see Fig. 1 of Jacoby 1989). Thus, in order to see PNs descended from young stars, a substantial Population I component is needed. This is unlikely for a normal elliptical galaxy, although a population of intermediate-mass progenitors with ages of ∼3 Gyr may explain the existence of objects $\lesssim 0.2$ mag brighter than M^*.

Coalesced binaries.—Iben & Tutukov (1989) have pointed out that ∼15% of all planetary nebulae should be formed during the interaction of close binary stars. For these objects, the expected mass distribution of central stars is distorted. Some PNs will end up with anomalously low-mass cores, as a result of aborted core evolution during the common envelope phase. Alternatively, if the spiral-down of a common envelope binary is extreme, the two components may merge and create a high-mass core. Yungelson, Tutukov, & Livio (1993) have estimated that this latter scenario will typically produce central stars in the range of 0.75–0.80 $M_\odot$—exactly that required for the overluminous objects. There is strong evidence that at least ∼15% of Galactic planetaries do indeed descend from a common envelope stage of evolution (Bond 1989; Bond & Livio 1990), and at least two planetary nebula central stars (EGB 5 and PHL 932) have been proposed as being the products of coalescence (Méndez et al. 1988a, b). However, the problem of stellar evolution inside common envelopes is complex and poorly constrained; no unambiguous case for a coalesced binary exists, and no Milky Way counterpart of the overluminous objects is known.

Chance superposition of PNs.—Figure 7 of Ciardullo et al. (1991) illustrates that the superposition of two fainter PNs can lead to the identification of an "overluminous" source. In that example, two bright PNs in the S0 galaxy NGC 1023 combined to create an object that was apparently overluminous by ∼0.3 mag. It was only when the seeing became 0".8 that the two sources could be resolved. Statistical experiments show that these coincidences should occur often enough to enhance the PNLF in the luminosity range 0.1–0.2 mag beyond M^* (Jacoby, Ciardullo, & Ford 1990). We intentionally exclude this luminosity range from our definition of overluminous objects partly for this reason. However, superpositions cannot explain sources more luminous than ∼0.4 mag beyond M^*, nor are they reasonable candidates for the distant halo objects. In addition, spectroscopy of PN 1 in NGC 4486 shows only a single emission line at 5007 Å. If superposition is at work here, the unlikely condition must be that both objects have the same radial velocity.

Background quasars.—Quasars with $z \sim 3.1$ will have their Lyα emission redshifted into the 5007 Å filter bandpass. To be identified as a PN candidate, though, the continuum emission must be suppressed by ∼3 mag below the emission-line flux. While unlikely, this possibility can only be excluded for PN 1 in NGC 4486, where spectroscopy demonstrates that the emission line is, indeed, [O III] λ5007.

5.2. *Revising the Empirical PNLF*

As stated above, the existence of overluminous [O III] λ5007 sources in a sample of planetary nebulae causes a problem for the maximum-likelihood method. Because the empirical law of equation (2) makes no provision for objects brighter than M^*, the presence of even one such source can distort the results from the fit. If a PN candidate is sufficiently overluminous, its exclusion from the sample can be justified on the basis of the resulting fit (i.e., the most-likely PNLF solution is excluded by a χ^2 or Kolmogorov-Smirnov statistic). However, an object that is $\sim$0.2 mag overluminous cannot be excluded in this way, and, depending on the circumstances, its inclusion in the sample may change the derived distance to a galaxy by $\sim$10%.

There is no statistically correct way to handle overluminous sources. If the luminosity function of these objects were known, *and* if the function were the same in every galaxy, then the empirical PNLF could be modified easily to include their contribution. Unfortunately, the rarity and uncertain origin of the phenomenon prevents us from knowing either of these things. In fact, in contrast to the luminosity function of normal planetary nebulae, there is good reason to believe that the luminosity function of overluminous objects is *not* the same in every galaxy. NGC 4278, which is a small elliptical, has two PN candidates that might qualify as overluminous; NGC 4494, which has 7 times more normal PNs than 4278, has none. Similarly, the giant ellipticals of Fornax, NGC 1399, 1316, and 1404, contain no overluminous PNs, while NGC 4374 and 4406 in Virgo have two each. Whether this variation is due to differences in stellar population or interstellar medium, the fact remains that the number of overluminous sources in a galaxy does not scale with the population of normal PNs, nor does it scale with any obvious galaxy property (e.g., luminosity or color).

The problems presented by the existence of overluminous objects can be illustrated by modifying the empirical PNLF in order to take into account the occasional appearance of interlopers. Assuming the luminosity function of contaminating objects is flat, we can express the observed luminosity function of all [O III] λ5007 sources as

$$N(M) \propto K + e^{0.307M}[1 - e^{3(M^*-M)}] \,, \quad \text{if } M > M^* \,,$$
$$N(M) \propto K \,, \quad \text{if } (M^* - 1) < M < M^* \,, \tag{3}$$

where K represents the nonzero likelihood of finding a contaminating source in any given magnitude interval. Given that between 1% and 2% of all extragalactic PNs brighter than $M_{5007} = -4.0$ are overluminous, $K \sim 0.005$.

If this formulation were applied to the PNs (and overluminous objects) of NGC 4278, the best-fitting distance to the galaxy would be almost $\sim$0.3 mag smaller than the nominal value of $(m - M)_0 = 30.04$. Moreover, the error on this distance would be a full $\sim$0.4 mag, or 3 times larger than the present error estimate. This change in the character of the solution comes from the normalization of K: in order to fit a PNLF, in which $\sim$30% of the bright PNs are overluminous, K has to be an order of magnitude larger. Without this large value of K, the PNLF cutoff is forced to brighter magnitudes and the estimated uncertainty is increased by the large number of (equally bad) solutions. It is possible, of course, to artificially increase K in order to compensate for the relatively large number of background contaminants (and this does recover the original distance modulus), but solutions with this added variable are ill defined. This is especially true with the small sample sizes frequently encountered in planetary nebula surveys.

The best way to correct for overluminous objects, of course, is to exclude them ahead of time, using their Hα emission or spatial extent. As Table 10 illustrates, one-third of the overluminous objects discovered to date are resolvable in good seeing, and, at least one other is bright in Hα. Thus, every attempt should be made to throw out possible contaminants a priori. If this cannot be done, then the safest approach is to compute the PNLF distances with and without the suspect interlopers and to include the two different results when computing the total uncertainty in the PNLF distance.

6. CONCLUSIONS

Our primary motivation for studying the Coma I group of galaxies was to test for a Hubble type dependence in the PNLF technique via internal (PNLF vs. PNLF) and external (PNLF vs. SBF vs. GCLF) comparisons. Somewhat surprisingly, our data, and that of the SBF and GCLF methods, suggest that the galaxies of the group are not all at a common distance. This has compromised the value of an internal test. However, external comparisons of PNLF distances against distances derived from the SBF and GCLF methods are still valuable. We find the following:

1. The PNLF, GCLF, and SBF methods place the E1 galaxy NGC 4494 2–4 Mpc more distant than the edge-on spiral NGC 4565. The separation is smallest for the PNLF method, so if one wants to attribute the difference in distance to a Hubble type dependence, the bias is smallest for the PNLF. We are not aware of any other technique that places these two galaxies closer together than $\sim$2 Mpc. Indeed, we are not aware of any other method that provides a measurement to both systems. There are few techniques that can be applied across such a wide range in Hubble types.
2. The PNLF distances to the E1 galaxy NGC 4278 and the Sb galaxy 4565 are essentially identical. If we had chosen to test the PNLF method with only these two galaxies, we would have concluded that there is no Hubble type dependence. That was the result we found in the NGC 1023 group. Thus, it is evident that larger samples of galaxies are required to detect the presence of systematic biases in PNLF distances (or those from any other technique) at the low levels (5%–10%) we are probing.
3. The PNLF, GCLF, and SBF techniques continue to yield consistent results at the 5%–10% level. Agreement for all three methods to the edge-on Sb galaxy, NGC 4565, is superb, having a sample dispersion of only $\pm$ 4%. This is rather remarkable, considering that all three methods are more commonly applied to early-type systems. For NGC 4494, the dispersion is 7%, still excellent by the standards of the field.

In addition, we find evidence that the luminosity function for overluminous [O III] sources is highly variable from galaxy to galaxy. This is not too surprising, considering that we identify eight plausible origins for these very rare (11) sources. We note that nearly half the sources classified as overluminous can be rejected as PNs either on the basis of their size (resolved objects are larger than $\gtrsim$25 pc, and consequently, are too large to be PNs) or their line ratios (bright PNs must be high-excitation objects). Thus, in cases of ambiguity, high-resolution imaging or imaging at other wavelengths can be used to exclude many interlopers.

We have attempted to refine our measurement algorithms to accommodate the low probability of overluminous sources contaminating the PNLF. Unfortunately, the lack of a known or constant luminosity function for these sources renders the prescription of limited value. Overluminous [O III] sources are rare, however, and usually they fall sufficiently off the nominal PNLF to be rejected as outliers during the fitting process. Consequently, they have little or no impact on PNLF distances.

R. C. was supported in part by NASA grant NAGW-3159 and NSF grant AST 92-57833. W. E. H. acknowledges financial support from the Natural Sciences and Engineering Research Council of Canada. We wish to thank Karen Kwitter and Phil Massey for helpful discussions regarding Wolf-Rayet nebulae, and Sidney van den Bergh for helpful suggestions to improve the presentation of this paper.

REFERENCES

Bertola, F. 1964, PASP, 76, 241
Bond, H. E. 1989, in IAU Symp. 131, Planetary Nebulae, ed. S. Torres-Peimbert (Dordrecht: Kluwer), 251
Bond, H. E., & Livio, M. 1990, ApJ, 355, 568
Brown, T., Cordova, F., Ciardullo, R., Thompson, R., & Bond, H. 1994, ApJ, 422, 118
Burstein, D., Bertola, F., Buson, L. M., Faber, S. M., & Lauer, T. R. 1988, ApJ, 328, 440
Burstein, D., & Heiles, C. 1984, ApJS, 54, 33
Burstein, D., Krumm, N., & Salpeter, E. E. 1987, AJ, 94, 883
Chu, Y. H. 1993, in IAU Symp. 155, Planetary Nebulae, ed. R. Weinberger & A. Acker (Dordrecht: Kluwer), 139
Ciardullo, R., Ford, H. C., Neill, J. D., Jacoby, G. H., & Shafter, A. W. 1987, ApJ, 318, 520
Ciardullo, R., Jacoby, G. H., & Feldmeier, J. 1996, in preparation
Ciardullo, R., Jacoby, G. H., & Ford, H. C. 1989a, ApJ, 344, 715
Ciardullo, R., Jacoby, G. H., Ford, H. C., & Neill, J. D. 1989b, ApJ, 339, 53
Ciardullo, R., Jacoby, G. H., & Harris, W. E. 1991, ApJ, 383, 487
Ciardullo, R., Jacoby, G. H., & Tonry, J. L. 1993, ApJ, 419, 479
Cohen, M., & Barlow, M. J. 1975, Astrophys. Lett., 16, 165
Cowley, A. P., Schmidtke, P. C., Crampton, D., & Hutchings, J. B. 1990, ApJ, 350, 288
Crawford, I. A., & Barlow, M. J. 1991, A&A, 249, 518
Davies, R. L., & Birkinshaw, M. 1988, ApJS, 68, 409
de Vaucouleurs, G. 1958, ApJ, 127, 487
———. 1975, in Stars and Stellar Systems IX, Galaxies and the Universe, ed. A. Sandage, M. Sandage, & J. Kristian (Chicago: Univ. Chicago Press), 557
de Vaucouleurs, G., de Vaucouleurs, A., Corwin, H. G., Jr., Buta, R. J., Paturel, G., & Fouqué, P. 1991, Third Reference Catalog of Bright Galaxies (New York: Springer) (RC3)
Di Stefano, R., Paerels, F., & Rappaport, S. 1995, ApJ, 450, 705
Dorman, B., Rood, R. T., & O'Connell, R. W. 1993, ApJ, 419, 596
Esteban, C., Vílchez, J. M., Smith, L. J., & Manchado, A. 1991, A&A, 244, 205
Feldmeier, J., Ciardullo, R., & Jacoby, G. H. 1996, ApJ, 461, in press
Ferguson, H. C., & Davidsen, A. F. 1993, ApJ, 408, 92
Fleming, D. B., Harris, W. E., Pritchet, C. J., & Hanes, D. A. 1995, AJ, 109, 1044
Freedman, W. L., & Madore, B. F. 1990, ApJ, 365, 186
Frogel, J. A., Persson, S. E., Aaronson, M., & Matthews, K. 1978, ApJ, 220, 75
Greggio, L., & Renzini, A. 1990, ApJ, 364, 35
Hamuy, M., Phillips, M. M., Maza, J., Suntzeff, N. B., Schommer, R. A., & Avilés, R. 1995, AJ, 109, 1
Hui, X., Ford, H. C., Ciardullo, R., & Jacoby, G. H. 1993, ApJ, 414, 463
Iben, I., & Tutukov, A. V. 1989, in IAU Symp. 131, Planetary Nebulae, ed. S. Torres-Peimbert (Dordrecht: Kluwer), 505
Jacoby, G. H. 1989, ApJ, 339, 39
———. 1995, in Science With the VLT, ed. J. Walsh & I. J. Danziger (Berlin: Springer), 267
Jacoby, G. H., Ciardullo, R., & Ford, H. C. 1990, ApJ, 356, 332
Jacoby, G. H., Ciardullo, R., Ford, H. C., & Booth, J. 1989, ApJ, 344, 704
Jacoby, G. H., Quigley, R. J., & Africano, J. L. 1987, PASP, 99, 672
Jacoby, G. H., Branch, D., Ciardullo, R., Davies, R. L., Harris, W. E., Pierce, M. J., Pritchet, C. J., Tonry, J. L., & Welch, D. L. 1992, PASP, 104, 599
Jedrzejewski, R., & Schechter, P. L. 1989, AJ, 98, 147
Johnson, H. L. 1966, ApJ, 143, 187
Kelson, D. D., et al. 1994, BAAS, 26, 1352
Kennicutt, R. C. 1984, ApJ, 287, 116
Kwok, S. 1983, in IAU Symp. 103, Planetary Nebulae, ed. D. R. Flower (Dordrecht: Reidel), 293
Lees, J. F. 1992, Ph.D. thesis, Princeton Univ.
Massey, P. 1981, ApJ, 246, 153
McClure, R. D., & Racine, R. 1969, AJ, 74, 1000
McMillan, R., Ciardullo, R., & Jacoby, G. H. 1993, ApJ, 416, 62
Méndez, R. H., Groth, H. G., Husfeld, D., Kudritzki, R. P., & Herrero, A. 1988a, A&A, 197, L25
Méndez, R. H., Kudritzki, R. P., Herrero, A., Husfeld, D., & Groth, H. G. 1988b, A&A, 190, 113
Minkowski, R. 1946, PASP, 58, 305
Oke, J. B. 1974, ApJS, 27, 21
Pakull, M. W., Ilovaisky, S., & Chevalier, C. 1985, Space Sci. Rev., 40, 229
Peimbert, M. 1990, Rev Mexicana Astron. Af., 20, 119
Peletier, R. F., Davies, R. L., Illingworth, G. D., Davis, L. E., & Cawson, M. 1990, AJ, 100, 1091
Raimond, E., Faber, S. M., Gallagher, J. S., III, & Knapp, G. R. 1981, ApJ, 246, 708
Rappaport, S., Di Stefano, R., & Smith, J. D. 1994, ApJ, 426, 692
Remillard, R., Rappaport, R., & Macri, L. 1995, ApJ, 439, 646
Seaton, M. J. 1979, MNRAS, 187, 73P
Shafter, A. W., Ciardullo, R., & Pritchet, C. J. 1996, in preparation
Simard, L., & Pritchet, C. J. 1994, AJ, 107, 503
Soffner, T., Méndez, R. H., Jacoby, G. H., Ciardullo, R., Roth, M. M., & Kudritzki, R. P. 1996, A&A, 306, 9
Stetson, P. B. 1987, PASP, 99, 191
Stone, R. P. S. 1977, ApJ, 218, 767
Tanvir, N. R., Shanks, T., Ferguson, H. C., & Robinson, D. R. T. 1995, Nature, 377, 27
Tonry, J. L., & Davis, M. 1981, ApJ, 246, 680
Tully, R. B., & Shaya, E. J. 1984, ApJ, 281, 31
van den Bergh, S., & McClure, R. D. 1994, ApJ, 425, 205
van den Bergh, S., & Tammann, G. A. 1991, ARA&A, 29, 363
van der Hucht, K. A., Jurriens, T. A., Olnon, F. M., Thé, P. S., Wesselius, P. R., & Williams, P. M. 1985, A&A, 145, L13
Wang, Q. 1991, MNRAS, 252, 47P
Weidemann, V. 1987, A&A, 188, 74
Welch, D. L., McAlary, C. W., McLaren, R. A., & Madore, B. F. 1986, ApJ, 305, 583
Yungelson, L. R., Tutukov, A. V., & Livio, M. 1993, ApJ, 418, 794